



**HAL**  
open science

## Unusual solvent dependence of a molecule-based FeII macrocyclic spin-crossover complex

Hongfeng Wang, Chiara Sinito, Abdellah Kaiba, José Sánchez Costa, Cédric Desplanches, Philippe Dagault, Philippe Guionneau, Jean-Francois Létard, Philippe Negrier, Denise Mondieig

► **To cite this version:**

Hongfeng Wang, Chiara Sinito, Abdellah Kaiba, José Sánchez Costa, Cédric Desplanches, et al.. Unusual solvent dependence of a molecule-based FeII macrocyclic spin-crossover complex . European Journal of Inorganic Chemistry, 2014, 2014 (29), pp.4927-4933. 10.1002/ejic.201402666 . hal-01075363

**HAL Id: hal-01075363**

**<https://hal.science/hal-01075363>**

Submitted on 8 Jan 2018

**HAL** is a multi-disciplinary open access archive for the deposit and dissemination of scientific research documents, whether they are published or not. The documents may come from teaching and research institutions in France or abroad, or from public or private research centers.

L'archive ouverte pluridisciplinaire **HAL**, est destinée au dépôt et à la diffusion de documents scientifiques de niveau recherche, publiés ou non, émanant des établissements d'enseignement et de recherche français ou étrangers, des laboratoires publics ou privés.



Distributed under a Creative Commons Attribution - NonCommercial - ShareAlike 4.0 International License

# Unusual Solvent Dependence of a Molecule-Based Fe<sup>II</sup> Macrocyclic Spin-Crossover Complex

Hongfeng Wang,<sup>[a,b]</sup> Chiara Sinito,<sup>[a,b]</sup> Abdellah Kaiba,<sup>[a,b]</sup>  
José Sanchez Costa,<sup>[a,b]</sup> Cédric Desplanches,<sup>\*[a,b]</sup>  
Philippe Dagault,<sup>[a,b]</sup> Philippe Guionneau,<sup>[a,b]</sup>  
Jean-François Létard,<sup>[a,b]</sup> Philippe Negrier,<sup>[c,d]</sup> and  
Denise Mondieig<sup>[c,d]</sup>

**Keywords:** Iron / Magnetic properties / Spin crossover / Phase transitions / Solvent effects / Dehydration

This work illustrates in detail the reversible hydration–dehydration process of a molecule-based material, which involves a drastic change of the switchable magnetic properties of the sample. Concretely, the complex [FeL<sub>222</sub>N<sub>3</sub>O<sub>2</sub>(CN)<sub>2</sub>]·H<sub>2</sub>O exhibits a spin crossover (SCO) accompanied by a change of the coordination number. The dehydration and rehydration of this SCO complex was carried out and monitored by different methods, which include X-ray diffraction analysis. The corresponding samples display a thermal spin transition as

well as a thermal quenching of the metastable high-spin state at low temperature. In particular it was observed that the rehydrated material exhibits a particularly high temperature of relaxation,  $T(\text{TIESST})$ , of the metastable high-spin state. On the other hand, it was shown that this compound exhibits a uncommon correlation between  $T(\text{TIESST})$  and the thermal SCO, as compared with other spin-crossover compounds that do not exhibit a change in coordination number.

## Introduction

Bistable materials have been widely studied, most notably, for their potential application in data storage.<sup>[1]</sup> Many examples of bistable behavior exist in Fe<sup>II</sup> spin-crossover (SCO) compounds.<sup>[2]</sup> Among those examples, complexes exhibiting the excited-spin-state-trapping phenomenon (either light-induced, i.e., LIESST effect,<sup>[3]</sup> or thermally induced, i.e., TIESST effect<sup>[4]</sup>) are very promising, because they can appear in a different spin state at a given temperature, depending on their thermodynamic history (memory effect). At low temperature, those Fe<sup>II</sup> complexes are in a stable low-spin (LS, <sup>1</sup>A<sub>1</sub>) state, whereas upon an external stimulus, that is, light irradiation or fast cooling, a metastable high-spin (HS, <sup>5</sup>T<sub>2</sub>) state can be reached. One of the limitations for applications based on this switching property is the stability of the metastable HS state over time. Above a limiting temperature, that is,  $T(\text{LIESST})$  or  $T(\text{TIESST})$ ,<sup>[5]</sup> the meta-

stable HS state decays within seconds or less, and this is too fast for most of the envisaged applications. Consequently, one general goal of studies on switchable materials is to get high values for  $T(\text{LIESST})$  or  $T(\text{TIESST})$ . The record of the highest  $T(\text{LIESST})$  or  $T(\text{TIESST})$  value today is found in a 3D cobalt–iron Prussian blue analogue with a value of about 180 K.<sup>[6,7]</sup> To overcome this limitation, the mechanism of the corresponding physical phenomenon must be explored. In particular, it has been attempted to identify the factors responsible for stabilizing the metastable state.<sup>[7,8]</sup> The main factor that strongly influences the metastability is the degree of coordination and the distortion of the metal coordination sphere in the HS state.<sup>[8,9]</sup> Concurrently, modifications of solvent and anion have been investigated in N<sub>6</sub> coordination complexes<sup>[9b,10]</sup> to stabilize the metastable HS state. Those modifications demonstrate that the factors of solvent and anion indirectly affect the degree of coordination in the cases of N<sub>6</sub> coordination complexes, and therefore, the roles of solvent and anion must be further explored. In this article, we focus on the Fe<sup>II</sup> macrocyclic complex [Fe(L<sub>222</sub>N<sub>3</sub>O<sub>2</sub>)(CN)<sub>2</sub>]·H<sub>2</sub>O {L<sub>222</sub>N<sub>3</sub>O<sub>2</sub> = 3,12,18-triaza-6,6-dioxabicyclo[12.3.1]octadeca-1(18),2,12,14,16-pentaene}. This complex holds a unique position in the panel of available spin-crossover materials, because to date it exhibits the highest  $T(\text{LIESST})$  observed for an iron(II) SCO material (135 K), and because it is the only known example of a SCO that involves a modification in coordination number.<sup>[10b,10c]</sup>

[a] CNRS, ICMCB, UPR 9048,  
33600 Pessac, France  
E-mail: desplanches@icmcb-bordeaux.cnrs.fr  
www.icmcb-bordeaux.cnrs.fr

[b] Univ. Bordeaux, ICMCB, UPR9048,  
33600 Pessac, France  
www.u-bordeaux.fr

[c] Univ. Bordeaux, LOMA, UMR 5798,  
33400 Talence, France

[d] CNRS, LOMA, UMR 5798,  
33400 Talence, France

The first evidence of the atypical magnetic properties of  $[\text{Fe}(\text{L}_{222}\text{N}_3\text{O}_2)(\text{CN})_2]\cdot\text{H}_2\text{O}$  was reported by Nelson et al.<sup>[11]</sup> Single-crystal X-ray diffraction analyses showed that this complex adopts a 7-coordinate HS state (HS-7,  $\text{FeN}_3\text{C}_2\text{O}_2$ )<sup>[12,13]</sup> at 293 K. At low temperature and depending on thermal history, two stable states can be achieved, that is, either a 6-coordinate LS state (LS-6,  $\text{FeN}_3\text{C}_2\text{O}$ )<sup>[14]</sup> or a 1:1 mixture HS-7 and LS-6 state (vide infra). LIESST experiments at the two stable states result in different stability of the metastable HS state: the  $T(\text{LIESST})$  value reaches 132 K when irradiation is performed on the LS-6,  $\text{FeN}_3\text{C}_2\text{O}$ , state. When irradiation is performed on the mixed state, the  $T(\text{LIESST})$  value only reaches 73 K.<sup>[15]</sup> On the other hand, if the complex is flash-cooled from 293 to 10 K, a  $T(\text{TIESST})$  value of 135 K is obtained.<sup>[16]</sup> This is the highest value reported for a mononuclear  $\text{Fe}^{\text{II}}$  complex. Note that the  $T(\text{LIESST})$  and  $T(\text{TIESST})$  values refer to well-defined and already reported experimental protocols to avoid small differences arising from different experimental choices.<sup>[5,17]</sup> Another particularity of this material is that it contains water molecules that contribute to the crystal cohesion. The determination of the effect of the water molecules on the switchable properties of this material is the goal of the present study.

In general, previous studies<sup>[9b,10b,10c,18]</sup> have shown that the solvent of crystallization has a tremendous effect on both  $T_{1/2}$  and  $T(\text{LIESST})$ . The nature of the solvent molecule and the degree of solvation are of importance. For example, in  $[\text{Fe}(\text{bpp})_2]\text{Br}_2\cdot 6\text{H}_2\text{O}$ ,  $T_{1/2}$  and  $T(\text{LIESST})$  are 340 and 40 K, respectively, whereas they are 252 and 77 K for the dehydrated compound  $[\text{Fe}(\text{bpp})_2]\text{Br}_2$ . Similarly, the values for  $T_{1/2}$  and  $T(\text{LIESST})$  are 288 and 70 K for  $[\text{Fe}(\text{bpp})_2](\text{BF}_4)_2\cdot 3\text{H}_2\text{O}$ , whereas they are 176 and 110 K for  $[\text{Fe}(\text{bpp})_2](\text{BF}_4)_2$ . In both cases, the dehydration induced a decrease of  $T_{1/2}$  and, more important, an increase of  $T(\text{LIESST})$ . To this extend, the dehydration of the studied complex  $[\text{Fe}(\text{L}_{222}\text{N}_3\text{O}_2)(\text{CN})_2]\cdot\text{H}_2\text{O}$  is of interest, because it already exhibits a high  $T(\text{LIESST})$ . Consequently, we thus attempted to dehydrate it.

In this work, we studied the influence of dehydration and rehydration of  $[\text{Fe}(\text{L}_{222}\text{N}_3\text{O}_2)(\text{CN})_2]\cdot\text{H}_2\text{O}$  on its spin-cross-over properties. The thermal quenching of the metastable HS state was also examined.

## Results and Discussion

Thermogravimetric analyses (TGA) were performed on  $[\text{Fe}(\text{L}_{222}\text{N}_3\text{O}_2)(\text{CN})_2]\cdot\text{H}_2\text{O}$  to test the possibility of dehydration and to precisely determine the corresponding temperature range (Figure 1).

Figure 1 (a) shows the TGA curve for a fresh  $[\text{Fe}(\text{L}_{222}\text{N}_3\text{O}_2)(\text{CN})_2]\cdot\text{H}_2\text{O}$  sample. The mass loss process starts at around 320 K and ends at around 385 K. The total mass loss at 385 K is about 4.46% and corresponds to one water molecule (4.49%, calculated). After the first TGA measurement (recorded up to 430 K), the sample was left at ambient atmosphere for one month. Then, the experiment was re-

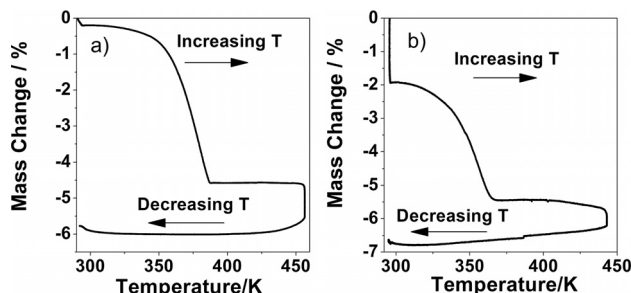


Figure 1. Thermogravimetric analyses (TGA) of (a) a freshly prepared  $[\text{Fe}(\text{L}_{222}\text{N}_3\text{O}_2)(\text{CN})_2]\cdot\text{H}_2\text{O}$  sample and (b) a sample left at ambient atmosphere for one month after an initial TGA treatment.

peated (Figure 1, b). The shape of the second TGA curve was different from the previous one, having two steps. The first step corresponds to a mass loss of around 1.9%, which occurs at 295 K under  $\text{N}_2$  flux of 3 h. The second step, which represents a mass loss of 3.53%, is associated with an increase of temperature up to 370 K. The mass loss for the second step corresponds to a main loss of 0.8 water molecules per complex. On the basis of previous studies,<sup>[12–14]</sup> it is reasonable to attribute the mass loss observed at room temperature to the water molecules adsorbed at the surface, whereas the behavior recorded during the heating process corresponds to 0.8 water molecules in the crystal lattice. From the crystallographic work performed on the  $[\text{Fe}(\text{L}_{222}\text{N}_3\text{O}_2)(\text{CN})_2]\cdot\text{H}_2\text{O}$  single crystals,<sup>[12–14]</sup> we have learned that the water molecules form hydrogen bonds with the two cyanido nitrogen atoms in the axial positions with an infinite 1D chain. The TGA experiments reveal that the water molecules in the lattice can be removed at high temperature. Thus, the hydrogen bonds between water molecules and nitrogen atoms are consequently broken. As a result, the 1D-chain character of the structure is lost. Rehydration may effectively reconstruct this chain. However, this reconstructed chain is certainly incomplete, because the mass loss observed by TGA is lower (loss of 0.8 water molecules) than for the original sample (loss of 1 water molecule).

A single crystal of  $[\text{Fe}(\text{L}_{222}\text{N}_3\text{O}_2)(\text{CN})_2]\cdot\text{H}_2\text{O}$  was mounted on a X-ray diffractometer, and the diffraction patterns were recorded at 293 K. The temperature was then increased to 333 K, and the diffraction patterns were re-recorded after 3 and 12 h of constantly keeping the crystal at 333 K. Diffraction patterns are presented in Figure 2.

Initially, the  $[\text{Fe}(\text{L}_{222}\text{N}_3\text{O}_2)(\text{CN})_2]\cdot\text{H}_2\text{O}$  diffraction pattern exhibits well defined spots at 293 K (Figure 2, a), as expected for a single crystal. When the single crystal is heated at 333 K, the diffraction pattern changes and reveals a phase transition (Figure 2, b). However, some diffraction rings also appear at the same time, which are attributed to the crystal becoming polycrystalline. Clearly visible after 2 h at 330 K, the rings already appear after a few minutes, and their intensity increases with time. After 12 h at 333 K, the initial diffraction Bragg peaks had totally disappeared. Any attempts to maintain the single-crystal character of the compound during heating were unsuccessful, and no struc-

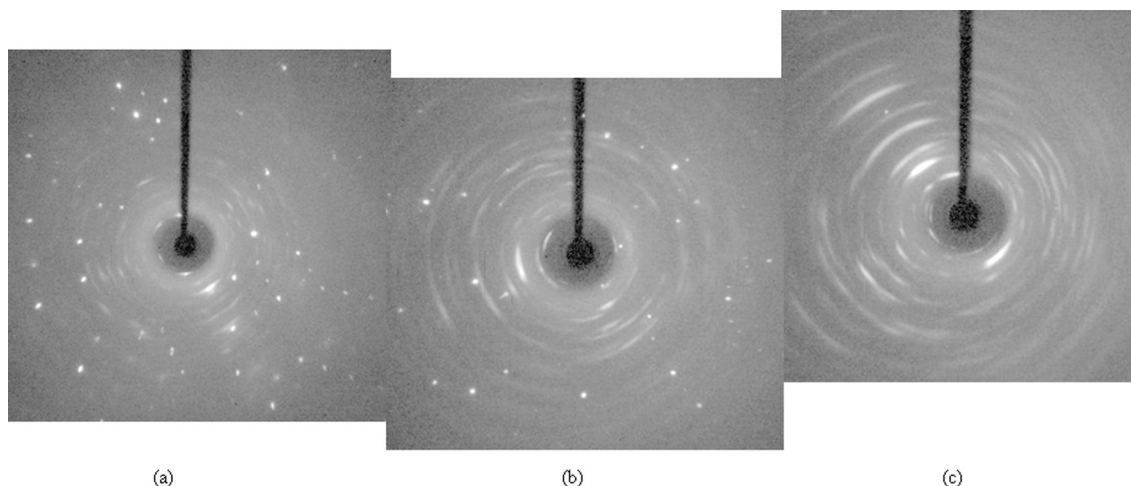


Figure 2. Diffraction pattern of a single crystal of  $[\text{FeL}_{222}\text{N}_3\text{O}_2(\text{CN})_2]\cdot\text{H}_2\text{O}$ , recorded at 293 K (a), after 2 h at 333 K (b), and after 12 h at 333 K (c).

ture determination of the high-temperature phase was successful with the single-crystal. Thus, powder X-ray diffraction (PXRD) was used to monitor the change of the diffraction pattern with temperature. PXRD patterns recorded between 303 and 403 K are reported in Figure 3.

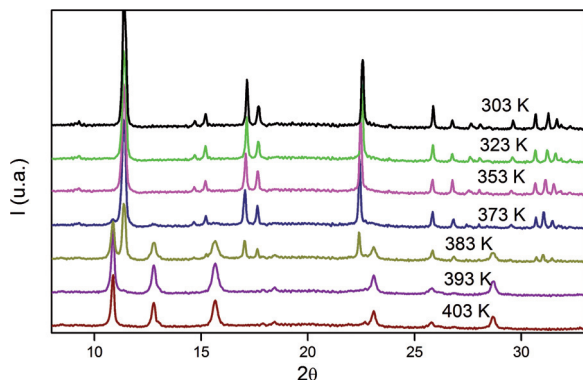


Figure 3. In situ PXRD patterns of compound  $[\text{FeL}_{222}\text{N}_3\text{O}_2(\text{CN})_2]\cdot\text{H}_2\text{O}$  at different temperatures.

The diffraction patterns at 303, 323, 353, and 373 K show peaks at the same diffraction angles. These peaks correspond to the diffraction pattern calculated from the known crystal structure of the hydrated compound  $[\text{Fe}(\text{L}_{222}\text{N}_3\text{O}_2)(\text{CN})_2]\cdot\text{H}_2\text{O}$ . At 383 K, new diffraction peaks appear. When the temperature was further increased to 393 K or 403 K, the diffraction pattern was completely modified. By comparison with the TGA measurements, the diffraction pattern at 403 K was attributed to the dehydrated compound. In the powder, the phase transition corresponding to dehydration is thus observed in the range 373–383 K. The difference compared to the temperature of the phase transition in the single crystal (around 330 K) is attributed to both the inherent differences in the experimental protocols and the nature (single crystal or powder) of the samples. It was possible to index the diffraction pattern of the dehydrated compound at 403 K (Figure 4).

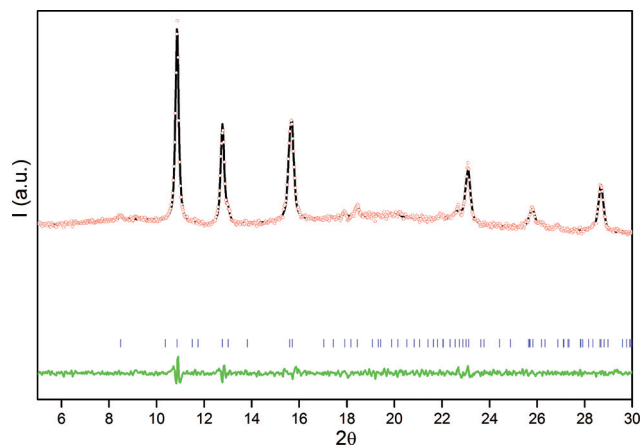


Figure 4. Refined PXRD pattern at 403 K. The observed and calculated values are drawn with red points and dark lines, respectively. Reflection positions are marked with vertical ticks, and the difference curve is shown at the bottom.

The dehydrated compound has a triclinic unit cell with the cell parameters  $a = 10.871(2) \text{ \AA}$ ,  $b = 9.387(2) \text{ \AA}$ ,  $c = 9.327(2) \text{ \AA}$ ,  $\alpha = 114.53(2)^\circ$ ,  $\beta = 106.464(7)^\circ$ , and  $\gamma = 86.32(2)^\circ$ , which results in a unit cell volume of  $V = 829(11) \text{ \AA}^3$ . These parameters can be compared with those of the hydrated compound, which crystallizes in the monoclinic space group  $C2/c$  with the parameters  $a = 17.326(5) \text{ \AA}$ ,  $b = 12.054(5) \text{ \AA}$ ,  $c = 10.125(5) \text{ \AA}$ ,  $\beta = 116.27(1)^\circ$ , which results in a unit cell volume of  $V = 1896.2(1) \text{ \AA}^3$ . The dehydration induces a phase transition corresponding to a loss of symmetry and to drastic modifications of the unit cell. The monoclinic unit cell contains 4 molecular complexes, which results in a volume of  $480 \text{ \AA}^3$  per complex. By comparison, the dehydrated unit cell corresponds to a volume of  $414 \text{ \AA}^3$  per molecular complex. Thus, the loss of water in the crystal structure corresponds to a strong decrease in volume (ca. 14%). A more detailed structural description cannot be given in absence of a full crystal structure determination. After the dehydration process, the

sample was left at ambient atmosphere for one month. The PXRD pattern was then recorded again and compared with the original one of  $[\text{Fe}(\text{L}_{222}\text{N}_3\text{O}_2)(\text{CN})_2]\cdot\text{H}_2\text{O}$  (Figure 5).

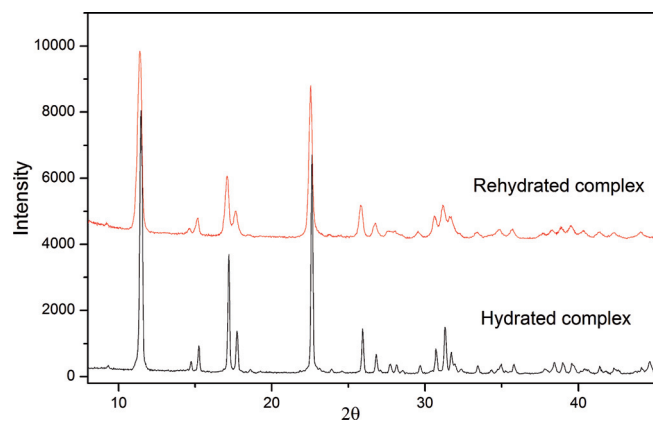


Figure 5. X-ray powder diffraction patterns of hydrated and rehydrated samples.

The diffraction patterns of the hydrated and rehydrated samples are very similar and show a global recovery of the initial crystal structure after the dehydration–rehydration process. However, it can be emphasized that the diffraction peaks observed after rehydration are significantly broadened, which is a sign of a loss of crystallinity in the compound. This is due to the fact that the dehydration–rehydration cycle has introduced some defects in the structure. These defects may be the origin of the different TGA behavior of the original and the rehydrated samples. Furthermore, if the compound is heated for 24 h at 390 K, the crystallinity is completely lost and cannot be recovered by leaving the compound at ambient atmosphere. This absence of reversibility points to an irreversible decomposition of the complex, although more detailed studies should be done to confirm this hypothesis.

IR absorption spectra were recorded for original and rehydrated compounds. No difference was noticed between the two spectra (see Supporting Information). This result agrees with the fact that the original and the rehydrated compounds have the same structure and that the difference between the two compounds is due to defects, which only result in a loss of crystallinity (vide supra).

To monitor the effect of the dehydration on the switchable properties through the corresponding magnetic behavior, in situ dehydration inside the SQUID chamber and rehydration in ambient atmosphere were performed to study the solvent dependence of the magnetic and photomagnetic properties. In situ dehydration was chosen, because it allows avoiding any contact of the compound with ambient atmosphere, preventing any partial rehydration. For dehydration, the sample was firstly placed at 380 K inside SQUID cavity for 90 min. Purging was performed during this time to remove the released water molecules. The temperature of 380 K was chosen in accordance to TGA and PXRD measurements, because this temperature allows for dehydration without decomposition of the compound. Magnetic mea-

surements were then performed between 300 and 10 K by firstly cooling the system and then heating it back at a rate of  $\pm 1.2 \text{ K min}^{-1}$ . The temperature dependence of the  $\chi_M T$  product ( $\chi_M$  is the molar magnetic susceptibility,  $T$  is the temperature) is plotted in Figure 6 (black squares). The high-temperature value of  $\chi_M T$  is  $3.08 \text{ cm}^3 \text{ mol}^{-1} \text{ K}$ , which is in good agreement with the value expected for a  $\text{Fe}^{\text{II}}$  ion in the HS state. Upon cooling,  $\chi_M T$  remains essentially constant down to approximately 140 K. Further cooling leads to a rapid decrease of  $\chi_M T$ , which reaches a value of  $0.85 \text{ cm}^3 \text{ mol}^{-1} \text{ K}$  at 70 K. Further cooling leads to no change in  $\chi_M T$ . Upon cooling, the spin transition occurs at  $T_{1/2 \downarrow} = 125 \text{ K}$ . On warming, the curve described by  $\chi_M T$  is essentially the same, but it is slightly shifted toward higher temperatures by about 5 K with a spin transition temperature of  $T_{1/2 \uparrow} = 130 \text{ K}$  and a thermal hysteresis of 5 K. Consequently, the dehydration corresponds to a strong modification of the spin-crossover features and leads to a decrease of  $T_{1/2}$  (by ca. 40 K) and a shortening of the hysteresis width.

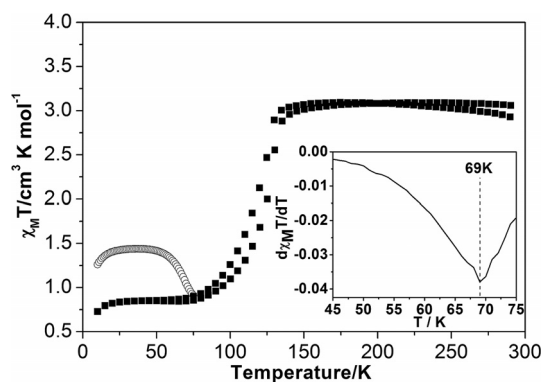


Figure 6. Temperature dependence of  $\chi_M T$  for  $[\text{Fe}(\text{L}_{222}\text{N}_3\text{O}_2)(\text{CN})_2]\cdot\text{H}_2\text{O}$  after dehydration at 380 K for 90 min inside SQUID chamber: (■) cooling and warming after dehydration, (○) TIESST experiment.

A TIESST experiment on the dehydrated compound was performed by following the standard procedure, that is, the sample was quench-cooled to 10 K, the temperature was then increased at  $0.3 \text{ K min}^{-1}$ , and  $\chi_M T$  was recorded simultaneously (Figure 6). Between 10 and 25 K,  $\chi_M T$  slightly increased from 1.25 to  $1.5 \text{ cm}^3 \text{ mol}^{-1} \text{ K}$ , and this increase is usually attributed to zero-field splitting. Between 25 and 50 K, the  $\chi_M T$  product remained almost constant at  $1.5 \text{ cm}^3 \text{ mol}^{-1} \text{ K}$ , which corresponds to a HS fraction of 0.5. Above 50 K,  $\chi_M T$  decreases, and at 75 K it reaches the curve recorded during slow cooling. The minimum of the derivative curve recorded after thermal quenching gives  $T(\text{TIESST})$ , which has a value of 69 K in this case (inset Figure 6).

After one month of rehydration in ambient atmosphere, the magnetic behavior of the previously dehydrated sample was re-investigated. The temperature dependence of  $\chi_M T$  is shown in Figure 7. Although the rehydrated sample is isomorphous with the original sample at 293 K (Figure 5), the transition behavior is different. Upon cooling, spin tran-

sition occurs around  $T_{1/2} \downarrow = 180$  K, and the  $\chi_M T$  values drop from  $3.34 \text{ cm}^3 \text{ mol}^{-1} \text{ K}$  at 213 K to  $1.94 \text{ cm}^3 \text{ mol}^{-1} \text{ K}$  at 130 K. Upon warming,  $T_{1/2} \uparrow = 210$  K is obtained, which results in a hysteresis width of 30 K. The spin-crossover curve of the rehydrated sample resembles the transition from the HS state (HS-7,  $\text{FeN}_3\text{C}_2\text{O}_2$ ) to a mixture of 50% HS and 50% LS state of the original, hydrated complex  $[\text{Fe}(\text{L}_{222}\text{N}_3\text{O}_2)(\text{CN})_2] \cdot \text{H}_2\text{O}$ , which was observed for the second cycle and subsequent ones. A previous study on a single crystal of the hydrated sample revealed that once the crystal broke, the spin transition preferably reaches this mixed state instead of the pure LS state (LS-6,  $\text{FeN}_3\text{C}_2\text{O}$ ) state.<sup>[12]</sup> Therefore, it is not surprising that the rehydrated sample, which has gone through reconstruction of the crystal packing, also prefers the same mixed state in the low-temperature region.

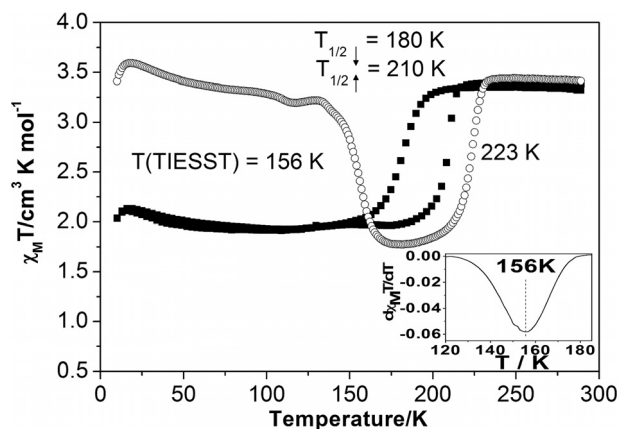


Figure 7. Temperature dependence of  $\chi_M T$  for  $[\text{Fe}(\text{L}_{222}\text{N}_3\text{O}_2)(\text{CN})_2] \cdot \text{H}_2\text{O}$  after rehydration in ambient atmosphere for one month: (■) cooling and warming after dehydration, (○) TIESST experiment.

For the rehydrated compound, the TIESST experiment was performed by following the same procedure as the one used for the dehydrated compound. A  $\chi_M T$  value of  $3.53 \text{ cm}^3 \text{ mol}^{-1} \text{ K}$  was obtained at 30 K, which indicates that approximately 100% of the metastable HS state can be reached. From the magnetic response, we obtained a  $T(\text{TIESST})$  value of 156 K. Taking into account that  $T(\text{TIESST})$  of the original, hydrated sample is 134 K, the reported value is a new record for a mononuclear  $\text{Fe}^{\text{II}}$  coordination complex. In Figure 7, we observe that the plot of the magnetic behavior after the  $T(\text{TIESST})$  experiment does not merge into the warming branch of the SCO curve for  $[\text{Fe}(\text{L}_{222}\text{N}_3\text{O}_2)(\text{CN})_2] \cdot \text{H}_2\text{O}$ , which is unusual. Instead, it reaches a  $\chi_M T$  value of  $1.77 \text{ cm}^3 \text{ mol}^{-1} \text{ K}$  at 180 K, which is lower than the value of  $1.97 \text{ cm}^3 \text{ mol}^{-1} \text{ K}$  of the SCO curve. Finally, a  $T_{1/2} \uparrow$  value of 223 K is obtained, and the curve merges into the SCO plot at 235 K. The difference of SCO and TIESST curve is possibly due to the fact that the metastable region of the complex is very close to the SCO region,<sup>[5b,5c]</sup> and therefore the kinetic effect reduced the spin-conversion process during the SCO measurement.

A  $T(\text{LIESST})$  database was initially developed to study the light-induced metastable state of  $\text{Fe}^{\text{II}}\text{N}_6$  SCO complexes. Now, it contains information about metastable states, no matter if they are light-induced or thermally trapped.<sup>[5b]</sup> The studied complexes include mononuclear  $\text{FeN}_6$ ,  $\text{Fe}^{\text{II}}$  phosphorus, and dinuclear  $\text{Fe}^{\text{II}}$  complexes, Prussian blue analogues, as well as  $\text{Fe}^{\text{III}}$  compounds. These complexes follow a general relationship:  $T(\text{LIESST}) = T_0 - 0.3T_{1/2}$ , where  $T_0$  is an empirical parameter that depends on the chemical nature of the ligands.  $T_0$  is 100, 120, 150, and 200 K for monodentate ligands, bidentate ligands, tridentate ligands, and solid 3D networks, respectively. In addition, one more group has been established for the compound studied in this paper, which has a macrocyclic ligand and  $T_0 = 180$  K. Until now,  $[\text{Fe}(\text{L}_{222}\text{N}_3\text{O}_2)(\text{CN})_2] \cdot \text{H}_2\text{O}$  is the only compound belonging to this  $T_0 = 180$  K line. As far as the influence of dehydration is concerned, the family of bpp [bpp = 2,6-bis(pyrazol-3-yl)pyridine] compounds has been widely studied. For example, the compounds  $[\text{Fe}(\text{bpp})_2](\text{BF}_4)_2 \cdot 3\text{H}_2\text{O}$ ,  $[\text{Fe}(\text{bpp})_2](\text{BF}_4)_2 \cdot 3\text{H}_2\text{O}$ ,  $[\text{Fe}(\text{bpp})_2] \cdot \text{Br}_2 \cdot 6\text{H}_2\text{O}$ , and  $[\text{Fe}(\text{bpp})_2]\text{Br}_2$ , whose  $T_{1/2}$  and  $T(\text{LIESST})$  have already been given in the introduction, align along the line of  $T_0 = 150$  K, as expected for the tridentate bpp ligand.<sup>[9]</sup> In particular, for these  $[\text{Fe}(\text{bpp})_2]^{2+}$  compounds, a decrease of  $T_{1/2}$  leads to an increase of  $T(\text{LIESST})$ . In contrast, dehydration of  $[\text{Fe}(\text{L}_{222}\text{N}_3\text{O}_2)(\text{CN})_2] \cdot \text{H}_2\text{O}$  clearly induces a decrease of both  $T_{1/2}$  and  $T(\text{TIESST})$ . This difference in behavior between  $[\text{Fe}(\text{L}_{222}\text{N}_3\text{O}_2)(\text{CN})_2] \cdot \text{H}_2\text{O}$  and other classical SCO compounds may be based on the fact that  $[\text{Fe}(\text{L}_{222}\text{N}_3\text{O}_2)(\text{CN})_2] \cdot \text{H}_2\text{O}$ , in addition to the classical spin transition observed in general and in the  $[\text{Fe}(\text{bpp})_2]^{2+}$  family in particular, exhibits a change in the coordination mode around the metal center.

## Conclusions

In situ PXRD reveals that a new phase of complex  $[\text{Fe}(\text{L}_{222}\text{N}_3\text{O}_2)(\text{CN})_2] \cdot \text{H}_2\text{O}$  is created by dehydration around 380 K. The dehydration phase adopts a triclinic unit cell that corresponds to a volume reduction of about 14%. However, the rehydration of this phase leads to a structure that is isomorphous with that of the original complex  $[\text{Fe}(\text{L}_{222}\text{N}_3\text{O}_2)(\text{CN})_2] \cdot \text{H}_2\text{O}$  at 293 K. By magnetic studies, it was demonstrated that the thermal SCO behaviors of the dehydrated and rehydrated samples were not identical, and they were both different from that of the original, hydrated complex. The thermal SCO of the dehydrated complex shows a spin transition around  $T_{1/2} \downarrow = 125$  K and  $T_{1/2} \uparrow = 130$  K, and  $T(\text{TIESST})$  is 69 K. However, the rehydrated sample shows a spin transition around  $T_{1/2} \downarrow = 180$  K and  $T_{1/2} \uparrow = 210$  K with  $T(\text{TIESST}) = 156$  K, compared to  $T(\text{TIESST}) = 135$  K of the original, hydrated material. This is the highest limiting temperature obtained for mononuclear  $\text{Fe}^{\text{II}}$  complexes to date. For this macrocyclic compound, the solvent dependence of  $T(\text{TIESST})$  does not follow the usual correlation with  $T_{1/2}$ . The new solvent dependence observed in this complex is probably linked to the

unusual change of coordination number during SCO, and it allows pushing the long-lived metastable HS state towards higher temperatures. This observation may open up new paths to reaching room-temperature phenomena.

## Experimental Section

**Thermogravimetric Analysis:** TGA curves were recorded with a Setaram MTB10–8 TGA apparatus. The sample was first left under a nitrogen flux for 3 h at room temperature, and then the temperature was increased up to 450 K with a rate of 1 K min<sup>-1</sup>. Later, the temperature was slowly decreased back to room temperature. The mass of the sample was continuously measured during the whole process.

**Infrared Spectra:** IR spectra were recorded with a Shimadzu IRAfinity-1 equipped with single-reflection horizontal ATR (HATR) MIRacle 10. To record the IR spectra of the rehydrated compound, the sample was first dehydrated under vacuum during 10 min at 100 °C and then left at ambient atmosphere during 10 h for rehydration.

**The Magnetic Properties:** The thermal spin transition was determined both in cooling and warming mode by measuring the magnetic susceptibility with a MPMS-55 Quantum Design SQUID magnetometer operating at approximately 2 Tesla in the range 10–290 K. These data are represented in the form of  $\chi_M T$ -vs- $T$  plots, where  $\chi_M$  is the molar magnetic susceptibility corrected for the diamagnetism of the closed-shell core and  $T$  is the temperature. In situ dehydration was performed inside the SQUID chamber at 380 K with continuous purging of with helium gas for 90 min. Thermal-trapping measurements were performed by following a published procedure. Samples were rapidly cooled to 10 K within one minute. Then, the temperature was increased at a rate of 0.3 K min<sup>-1</sup>. The  $T(\text{TIESST})$  temperature was estimated from the minimum of the derivative curve.

**Powder X-ray Diffraction:** Variable-temperature X-ray diffraction patterns were recorded with a horizontally mounted INEL cylindrical position-sensitive detector (CPS 120) operating by gas ionization (Argon + C<sub>2</sub>H<sub>6</sub>) by using Debye–Scherrer geometry (angular step ca. 0.029° – 2 $\theta$ ). Monochromatic Cu-K $\alpha$ 1 radiation was selected as the incident beam by means of a curved quartz monochromator. The generator power was set to 40 kV and 25 mA. Samples were introduced in 0.5 mm diameter Lindemann glass capillaries, and the latter rotated around its axis during the experiment to minimize preferential orientations of the crystallites. Data of hydrated and rehydrated compounds were recorded by using a PANalytical X'Pert MPD diffractometer with Bragg–Brentano geometry, Cu-K $\alpha$  radiation, and a backscattering graphite monochromator.

## Acknowledgments

The authors acknowledge financial support from the Agence Nationale de la Recherche (ANR) and the Conseil Régional d'Aquitaine.

- Bousseksou, G. Molnár, L. Salmon, W. Nicolazzi, *Chem. Soc. Rev.* **2011**, *40*, 3313; P. Gütllich, A. B. Gaspar, Y. Garcia, J. Beilstein, *Org. Chem.* **2013**, *9*, 342; G. Aromi, L. A. Barros, O. Roubeau, P. Gamez, *Coord. Chem. Rev.* **2011**, *255*, 485.
- [2] a) *Spin Crossover in Transition Metal Compounds*, in: *Topics in Current Chemistry* (Eds.: P. Gütllich, H. A. Goodwin), Springer-Verlag, Berlin, Heidelberg, New York, **2004**, vol. I, II, and III; b) *Spin-Crossover Materials: Properties and Applications* (Ed.: M. A. Halcrow), John Wiley & Sons, Hoboken, **2013**.
- [3] a) S. Decurtins, P. Gütllich, C. P. Köhler, H. Spiering, A. Hauser, *Chem. Phys. Lett.* **1984**, *105*, 1; b) A. Hauser, *Chem. Phys.* **1986**, *124*, 543; c) J. J. McGarvey, I. Lawthers, *J. Chem. Soc., Chem. Commun.* **1982**, 906.
- [4] a) G. Ritter, E. König, W. Irlner, H. A. Goodwin, *Inorg. Chem. Lett.* **1978**, *17*, 224; b) H. A. Goodwin, K. H. Sugiyarto, *Chem. Phys. Lett.* **1987**, *139*, 470; c) T. Buchen, P. Gütllich, H. A. Goodwin, *Inorg. Chem.* **1994**, *33*, 4573.
- [5] a) J.-F. Létard, P. Guionneau, L. Rabardel, J. A. K. Howard, A. E. Goeta, D. Chasseau, O. Kahn, *Inorg. Chem.* **1998**, *37*, 4432; b) N. Paradis, G. Chastanet, J.-F. Létard, *Eur. J. Inorg. Chem.* **2012**, 3618; c) N. Paradis, G. Chastanet, F. Varret, J.-F. Létard, *Eur. J. Inorg. Chem.* **2013**, 968; d) J.-F. Létard, G. Chastanet, P. Guionneau, C. Desplanches, *Optimizing the Stability of Trapped Metastable Spin States*, in: *Spin-Crossover Materials: Properties and Applications* (Ed.: M. A. Halcrow), Wiley, Oxford, UK, **2013**, chapter 19, p. 475.
- [6] D. Li, R. Clérac, O. Roubeau, E. Harte, C. Mathonière, R. Le Bris, S. M. Holmes, *J. Am. Chem. Soc.* **2008**, *130*, 252.
- [7] a) A. Hauser, *Coord. Chem. Rev.* **1991**, *111*, 275; b) A. Hauser, *Comments Inorg. Chem.* **1995**, *17*, 17; c) A. Hauser, C. Enaschescu, M. L. Daku, A. Vargas, N. Amstutz, *Coord. Chem. Rev.* **2006**, *250*, 1642.
- [8] a) M. Marchivie, P. Guionneau, J.-F. Létard, D. Chasseau, *Acta Crystallogr., Sect. B: Struct. Sci.* **2005**, *61*, 25; b) S. Alvarez, *J. Am. Chem. Soc.* **2003**, *125*, 6795; c) C. Boilleau, N. Suaud, N. Guihery, *J. Chem. Phys.* **2012**, *137*, 224304; d) M. Buron-Le-Cointe, J. Hébert, C. Baldé, N. Moisan, L. Toupet, P. Guionneau, J. F. Létard, H. Cailleau, E. Collet, *Phys. Rev. B* **2012**, *85*, 064114.
- [9] a) J.-F. Létard, L. Capes, G. Chastanet, N. Moliner, S. Létard, J. A. Real, O. Kahn, *Chem. Phys. Lett.* **1999**, *313*, 115; b) S. Marcén, L. Lecren, L. Capes, H. A. Goodwin, J.-F. Létard, *Chem. Phys. Lett.* **2002**, *358*, 87; c) J.-F. Létard, P. Guionneau, O. Nguyen, J. S. Costa, S. Marcén, G. Chastanet, M. Marchivie, L. Goux-Capes, *Chem. Eur. J.* **2005**, *11*, 4582; d) J.-F. Létard, *J. Mater. Chem.* **2006**, *16*, 2550.
- [10] a) V. Money, J. S. Costa, S. Marcen, G. Chastanet, J. Elhaïk, M. A. Halcrow, J.-F. Létard, *Chem. Phys. Lett.* **2004**, *391*, 273–277; b) M. A. Halcrow, *Chem. Soc. Rev.* **2011**, *40*, 4119; c) P. Guionneau, *Dalton Trans.* **2014**, 43, 382.
- [11] a) S. M. Nelson, P. D. A. Mellroy, C. S. Stevenson, E. König, G. Ritter, J. Waigel, *J. Chem. Soc., Dalton Trans.* **1986**, 991–995; b) E. König, G. Ritter, J. Dengler, S. M. Nelson, *Inorg. Chem.* **1987**, *26*, 3582.
- [12] S. Hayami, Z. Gu, Y. Einaga, Y. Kobayashi, Y. Ishikawa, Y. Yamada, A. Fujishima, O. Sato, *Inorg. Chem.* **2001**, *40*, 3240.
- [13] P. Guionneau, J. S. Costa, J.-F. Létard, *Acta Crystallogr., Sect. C* **2004**, *60*, m587.
- [14] P. Guionneau, F. Le Gac, A. Kaiba, J. S. Costa, D. Chasseau, J.-F. Létard, *Chem. Commun.* **2007**, 36, 3723.
- [15] J. S. Costa, P. Guionneau, J.-F. Létard, *J. Phys.: Conf. Ser.* **2005**, *21*, 67.
- [16] José Sánchez Costa, *Ph. D. Thesis*, Université Bordeaux I, **2005**.
- [17] M. Marchivie, P. Guionneau, J.-F. Létard, D. Chasseau, J. A. K. Howard, *J. Phys. Chem. Solids* **2004**, *65*, 17.
- [18] a) J. A. Real, A. B. Gaspar, V. Niel, M. C. Munoz, *Coord. Chem. Rev.* **2003**, *236*, 121; b) G. Lemerrier, N. Brefuel, S.

[1] a) O. Kahn, C. J. Martinez, *Science* **1998**, *279*, 44; b) C. Joachim, J. K. Gimzewski, A. Aviram, *Nature* **2000**, *408*, 541; c) J. K. Gimzewski, C. Joachim, *Science* **1999**, *283*, 1683; A.

Shova, J. A. Wolny, F. Dahan, M. Verelst, H. Paulsen, A. X. Trautwein, J.-P. Tuchagues, *Chem. Eur. J.* **2006**, *12*, 7421; c) M. Hostettler, K. W. Törnroos, D. Chernyshov, B. Vangdal, H.-B. Bürgi, *Angew. Chem. Int. Ed.* **2004**, *33*, 4589; *Angew. Chem.* **2004**, *116*, 4689; d) C.-F. Sheu, S. Pillet, Y.-C. Lin, S.-M. Chen,

I.-J. Hsu, C. Lecomte, Y. Wang, *Inorg. Chem.* **2008**, *47*, 10866; e) G. S. Matouzenko, E. Jeanneau, A. Y. Verat, Y. de Gaetano, *Eur. J. Inorg. Chem.* **2012**, 969.